

# Slope analysis for elastic nucleon-nucleon scattering

V.A. Okorokov <sup>a</sup>

Moscow Engineering Physics Institute (State University),  
Kashirskoe Shosse 31, 115409 Moscow, Russian Federation

date April 23, 2009

**Abstract.** The diffraction slope parameter is investigated for elastic proton-proton and proton-antiproton scattering based on the all available experimental data at low and intermediate momentum transfer values. Energy dependence of the elastic diffraction slopes is approximated by various analytic functions. The expanded "standard" logarithmic approximations with minimum number of free parameters allow to describe experimental slopes in all available energy range reasonably. The estimations of asymptotic shrinkage parameter  $\alpha'_P$  were obtained for various  $|t|$  domains based on the all available experimental data. Various approximations differ from each other both in the low energy and very high energy domains. Predictions for diffraction slope parameter are obtained for elastic proton-proton scattering at NICA, RHIC and LHC energies, for proton-antiproton elastic reaction in FAIR energy domain for various approximation functions.

**PACS.** 13.75.Cs Nucleon-nucleon interactions – 13.85.Dz Elastic scattering

## 1 Introduction

Elastic hadron-hadron scattering, the simplest type of hadronic collision process, remains one of the topical theoretical problems in fundamental interaction physics at present. Forward elastic scattering process is an excellent test for some fundamental principles (unitarity, analyticity, asymptotic theorems) of modern approaches. In the case of  $pp$  and  $\bar{p}p$  elastic scattering, although many experiments have been made over an extended range of initial energies and momentum transfer, these reactions are still not well understood. One can suggest that by the time the accelerator complexes like RHIC, LHC etc. are operating, the interest to the soft physics increases significantly. In the absence of a pure QCD description of the elastic  $pp/\bar{p}p$  and these large-distance scattering states (soft diffraction), an empirical analysis based on model-independent fits to the physical quantities involved plays a crucial role [1]. Therefore, empirical fits of energy dependencies of global scattering parameters have been used as an important source of the model-independent information. This approach for  $\sigma_{tot}$  and  $\rho$  was recently used in [2]. The third important quantity for nucleon elastic scattering is the slope parameter. The nuclear slope  $B$  for elastic scattering is of interest in its own right. This quantity defined according to the following equation:

$$B(s, t) = \frac{\partial}{\partial t} \left( \ln \frac{\partial \sigma(s, t)}{\partial t} \right), \quad (1)$$

is determined experimentally by fitting the differential cross section  $d\sigma/dt$  at some collision energy  $\sqrt{s}$ . On the other hand the study of  $B$  parameter is important, in particular, for reconstruction procedure of full set of helicity amplitudes for elastic nucleon scattering [2]. In the last 20-30 years, high-energy  $\bar{p}p$  colliders have extended the maximum  $\bar{p}p$  collision energy from  $\sqrt{s} \sim 20$  GeV to  $\sqrt{s} \sim 2$  TeV, the RHIC facility allows to obtain  $pp$  data up to  $\sqrt{s} = 500$  GeV<sup>1</sup>. As consequence, the available collection of  $pp$  and  $\bar{p}p$  slope data from literature has extended. The present status of slope for elastic  $pp$  and  $\bar{p}p$  scattering is discussed over the full energy domain. Predictions for further facilities are obtained based on the available experimental data.

## 2 Experimental slope energy dependence

We have attempted to describe the energy behavior of the elastic nuclear slopes for  $pp$  and  $\bar{p}p$  reactions. The classical Pomeron theory gives in first approximation the following expression for the differential cross section of elastic scattering at asymptotically high energies:

$$d\sigma/dt \propto s^{2(\alpha_P(t)-1)},$$

where  $\alpha_P(t)$  is a Pomeron trajectory. If  $\alpha_P(t)$  is linear function of momentum transfer, i.e.  $\alpha_P(t) = \alpha_P(0) + \alpha'_P t$ ,

<sup>1</sup> According to the RHIC Run plan the  $pp$  data at highest energy  $\sqrt{s} = 500$  GeV have to be collected during the spring – summer Run 2009.

<sup>a</sup> e-mail: VAOkorokov@mephi.ru; Okorokov@bnl.gov

then for the slope parameter  $B(s)$  at some  $t$  using the definition (1) one can obtain

$$B(s) \propto 2\alpha'_p \ln s.$$

Indeed the ensemble of experimental data on slopes for elastic nucleon collisions can be approximated reasonably by many phenomenological approaches, at least for  $\sqrt{s} > 20$  GeV. But models contradict the experimental data at lower energies and / or phenomenological approaches have a significant number of free parameters as usual. On the other hand it is apparent from previous investigations that the experimental data on slope parameters do not follow the straight lines at any initial energies when plotted as function of  $\ln s$ . The new "expanded" logarithmic parameterizations with small number of free parameters have been suggested in [2,3] for description of the elastic slope at all available energies. Thus taking into account standard Regge parametrization and quadratic function of logarithm from [4] the following analytic equations are under study here:

$$B(s, t) = B_0 + 2a_1 \ln(s/s_0), \quad (2a)$$

$$B(s, t) = B_0 + 2a_1 \ln(s/s_0) + a_2 [\ln(s/s_0)]^{a_3}, \quad (2b)$$

$$B(s, t) = B_0 + 2a_1 \ln(s/s_0) + a_2 (s/s_0)^{a_3}, \quad (2c)$$

$$B(s, t) = B_0 + 2a_1 \ln(s/s_0) + a_2 [\ln(s/s_0)]^2, \quad (2d)$$

where  $s_0 = 1$  GeV<sup>2</sup>, in general case parameters  $B_0$ ,  $a_i$ ,  $i = 1 - 3$  depend on range of  $|t|$  which is used for approximation. The function (2d) is a special case of (2b) at fixed value  $a_3 = 2$ . Additional terms in (2b) – (2d) take into account the non-logarithmic part of the energy dependence of the elastic nuclear slopes. Approximation function (2c) is analogy of parametrization of momentum slope dependence from [5]. One can see the parametrization (2c) is compatible to first order with the Regge pole model where the additional term represents the interference between the Pomeron and secondary trajectories [5].

Most of experimental investigations as well as theoretical models are focused on the diffraction region  $|t| \simeq 0-0.5$  GeV<sup>2</sup>. In this paper we study all available experimental data for nuclear slope parameter up to  $|t| \simeq 3.6$  GeV<sup>2</sup>. Experimental data are from [6,7,8,9,10,11]. The data sample consists of about 500 experimental points. The ensemble of experimental data has been slightly specified and improved in comparison with [3]. In particular, results obtained in [9] for form-factor parametrization of  $d\sigma/dt$  were included in the data sample after detail additional investigation. The total number of experimental points is equal 142/138 for  $pp/\bar{p}p$  scattering at low  $|t|$ , respectively. In the intermediate  $|t|$  domain experimental data set is 136/69 for  $pp/\bar{p}p$  reaction respectively. Thus the experimental sample is significantly larger than that for some early investigations [2,4,5,6,12]. The careful analysis of data sample allows to suggest that the influence of double counting in the experimental data is negligible. It should be emphasized that the experimental data for intermediate  $|t|$  range were separated on two samples which corresponded the various parametrization types for differential cross-section, namely, linear,  $\ln(d\sigma/dt) \propto (-B|t|)$ ,

and quadratic,  $\ln(d\sigma/dt) \propto (-B|t| \pm Ct^2)$ , function. Here  $B, C > 0$  are suggested. As known the measurements of nuclear slope, especially at intermediate  $|t|$  do not form a smooth set in energy, in contrast to the situation for global scattering parameters  $\rho$  and  $\sigma_{tot}$ , where there is a good agreement between various group data [4]. Detailed comparisons of slope data from different experiments are difficult because the various experiments cover different  $|t|$  ranges, use various fitting procedures, treat systematic errors in different ways, and, moreover, some experimental details are lost, especially, for very early data. We have tried to use as much as possible data for fitting from available samples. But some of the  $B$  values were not further used, either due to internal inconsistencies in the fitting procedure, or as redundant in view of a better determination at a nearby initial energy. Thus the data samples for approximations are somewhat smaller because of exclusion of points which, in particular, differ significantly from the other experimental points at close energies. Critical for a consistent determination of slope parameters is the choice of the range  $|t|_{\min} \leq |t| \leq |t|_{\max}$  over which the fit of  $d\sigma/dt$  is performed. It seems both the mean value of  $|t|$  ( $\bar{|t|}$ ) and  $|t|$ -boundaries of corresponding measurements are important for separation of experimental results on different  $|t|$  domains. Here the  $\bar{|t|}$  are calculated with taking into account approximations of experimental  $d\sigma/dt$  distributions instead of identifying of  $\bar{|t|}$  with mean point of  $|t|$ -range as previously [3]. Errors of experimental points include available clear indicated systematic errors added in quadrature to statistical ones. One need to emphasize the systematic errors caused by the uncertainties of normalization (total or/and differential cross sections) are not taken into account if these uncertainties are not included in the systematic errors in the original papers.

Let us describe the fitting algorithm in more detail. We use the fitting procedure with standard likelihood function for this investigation of nuclear slope parameter. In accordance with [12] let us define the quantity

$$\Delta\chi_i^2(s_i; \alpha) \equiv \left( \frac{B_m^i - B(s_i; \alpha)}{\sigma_i} \right)^2, \quad (3)$$

where  $B_m^i$  is the measured value of nuclear slope at  $s_i$ ,  $B(s_i; \alpha)$  is the expected value from the one of the fitting functions under consideration,  $\sigma_i$  is the experimental error of the  $i$ -th measurement. The parameters  $\alpha_j$  are given by the  $N$ -dimensional vector  $\alpha = \{\alpha_1, \dots, \alpha_N\}$ . Our fitting algorithm is some similar to the "sieve" algorithm from [12] with following modification. We reject the points which *a priori* differ significantly from other experimental data at close energies. The step allows us to get a first estimation of  $\chi^2/n.d.f.$  with minimum number of rejected points. The fit quality is improved at the next steps consequently. As indicated above smoothness of experimental slope energy dependence differs significantly for data samples in various  $|t|$ -domains and for various parameterizations of  $d\sigma/dt$  (see below). The  $\Delta\chi_i^2(s_i; \alpha)$  absolute value can be large for one data sample but it can be acceptable for another sample at the same time. Therefore we suggest to use the

relative quantity

$$n_\chi = \frac{\Delta\chi_i^2(s_i; \alpha)}{\chi^2/\text{n.d.f.}} \quad (4)$$

in order to reject the outliers (points far off from the fit curve to the data sample) instead of constant cut value  $\Delta\chi_i^2(s_i; \alpha)_{\max}$  from the "sieve" algorithm [12]. One needs to emphasize the fit function with best  $\chi^2/\text{n.d.f.}$  among (2a) – (2d) is used for expected value calculation in (3) at the each algorithm step. The points with  $n_\chi \geq n_\chi^{\max}$  are excluded from future study in our algorithm, where the  $n_\chi^{\max}$  is some empirical cut value. The conventional fit is made to the new "sifted" data sample. We consider the estimates of fit parameters as the final results if there are no excluded points for present data sample. We use the one value  $n_\chi^{\max} = 2$  for all data samples considered in this paper below. The fraction of excluded points is about 2% for  $pp$  as well as for  $\bar{p}p$  elastic scattering for low  $|t|$  domain. The maximum relative amount of rejected points is about 3%/12% for linear  $\ln d\sigma/dt$  parametrization and 6%/15% for quadratic one at intermediate  $|t|$  values for  $pp/\bar{p}p$  scattering respectively.

## 2.1 Low $|t|$ domain

The energy dependence for experimental slopes and corresponding fits by (2a) – (2d) are shown at Fig.1 and Fig.2 for  $pp$  and  $\bar{p}p$  correspondingly. The fitting parameter values are indicated in Table 1. One can see that the fitting functions (2a), (2d) describe the  $pp$  (Fig.1) and  $\bar{p}p$  (Fig.2) experimental data statistically acceptable only for  $\sqrt{s} \geq 5$  GeV. Additional study demonstrate that the extension of approximation domain to the lower energies for parameterizations (2a) and (2d) results in significant increasing of  $\chi^2/\text{n.d.f.}$  for  $\bar{p}p$  data. Thus these fit functions allow to get a statistically acceptable fit qualities only at  $\sqrt{s} \geq 5$  GeV for  $\bar{p}p$  scattering as well as for elastic  $pp$  reaction. The parameter  $a_1$  for Regge-inspired function (2a) is close to estimation for Pomeron parameter  $\alpha'_P \approx 0.25$  GeV<sup>-2</sup> for  $\bar{p}p$  data but this parameter is some larger than  $\alpha'_P$  estimate for proton-proton data. The  $a_1^{pp}$  value for (2a) from Table 1 is equal within the errors the early experimental estimations of "true" Pomeron shrinkage parameter [13]. The parameter  $a_1$  for function (2b) is equal within errors to the above estimation for Pomeron theory parameter  $\alpha'_P$  for  $pp$  data. The value of  $a_1^{pp}$  parameter for fitting function (2c) agrees with early value for similar fit of slope momentum dependence [5] but the present result is more precise than previous one. The RHIC point for proton-proton collisions has a large error and can't discriminate the approximations. Fitting functions (2b), (2c) allow us to describe experimental data at all energies with reasonable fit quality for  $pp$ . The functions (2a) – (2c) are close to each other at  $\sqrt{s} \geq 5$  GeV, especially, the Regge model approximation and (2c) fit. It seems the ultra-high energy domain is suitable for separation of various parameterizations. The qualities of (2b), (2c) approximations for  $\bar{p}p$  elastic scattering data are much poorer because of very sharp behavior

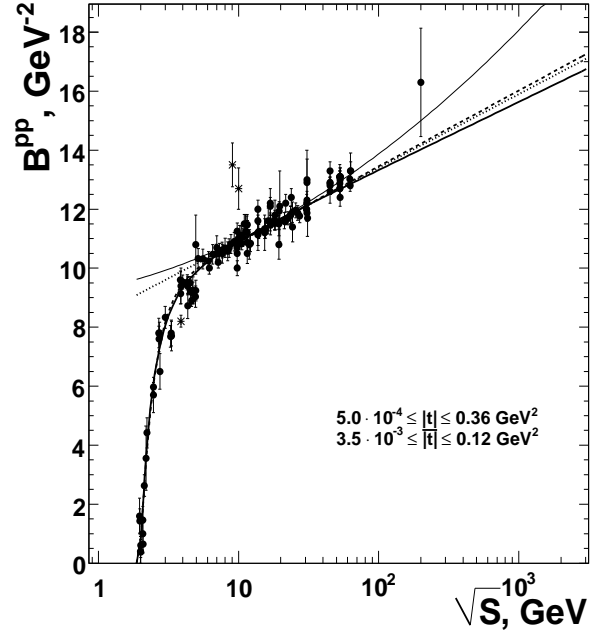


**Fig. 1.** Energy dependence of the elastic slope parameters for proton-proton scattering for low  $|t|$  domain. Experimental fitted points are indicated as  $\bullet$ , unfitted points are indicated as  $*$ . The curves correspond to the fitting functions as following: (2a) – dot, (2b) – thick solid, (2c) – dot-dashed, (2d) – thin

of experimental data near the low energy boundary. But one can see that the functions (2b), (2c) agree with experimental points at qualitative level and (very) close to each other for all energy range. The fit quality is some better for function (2b) than that for parametrization (2c) both for  $pp$  and  $\bar{p}p$  data. Additional study of antiproton-proton data shows that the increasing of low boundary of fit range ( $s_{\min}$ ) leads to the better fit quality for functions (2b), (2c) but at the same time, obviously, to the lost of some low-energy  $pp$  data. The fit quality changes dramatically at small increasing of  $s_{\min}$  from low boundary value  $4m_p^2$  to  $3.72$  GeV<sup>2</sup>. It was obtained  $\chi^2/\text{n.d.f.} \approx 5.4/5.5$  for function (2b) / (2c) respectively for fit range  $s_{\min} \geq 3.72$  GeV<sup>2</sup>. On the other hand the data sample is about 75% from maximum one in this case. Thus it seems the  $s_{\min} = 3.72$  GeV<sup>2</sup> one of the optimum values from point of view both fit quality and closing to the threshold  $s_{\min} = 4m_p^2$ . The average value of (3) for excluded points is equal 15.6 for  $pp$  and 649.8 for  $\bar{p}p$  data sample for parametrization (2b).

One can get predictions for nuclear slope parameter values for some facilities based on the results shown above. The  $B$  values at low  $|t|$  for different energies of FAIR, NICA, RHIC, and LHC are shown in the Table 2. As expected the functions (2b) and (2c) predicted very close slope parameter values for FAIR. The approximation function (2a) and (2d) can predict for  $\sqrt{s} \geq 5$  GeV only. Functions (2a) – (2c) predict much smaller values for  $B$  in high-energy  $pp$  collisions than (2d) approximation. Perhaps, the future more precise RHIC results will agree better with predictions based on experimental data fits under study.

**Table 1.** Fitting parameters for slope energy dependence in low  $|t|$  domain

Function	Parameter				
	$B_0, \text{GeV}^{-2}$	$a_1, \text{GeV}^{-2}$	$a_2, \text{GeV}^{-2}$	$a_3$	$\chi^2/\text{n.d.f.}$
proton-proton scattering					
(2a)	$8.41 \pm 0.08$	$0.271 \pm 0.007$	–	–	179/95
(2b)	$8.73 \pm 0.12$	$0.250 \pm 0.009$	$-28 \pm 2$	$-3.50 \pm 0.14$	349/135
(2c)	$8.31 \pm 0.08$	$0.279 \pm 0.007$	$-188 \pm 23$	$-2.24 \pm 0.09$	358/135
(2d)	$9.3 \pm 0.3$	$0.11 \pm 0.06$	$0.03 \pm 0.01$	–	171/94
proton-antiproton scattering					
(2a)	$10.0 \pm 0.2$	$0.215 \pm 0.012$	–	–	32/27
(2b)	$12.02 \pm 0.06$	$0.121 \pm 0.006$	$495 \pm 98$	$-13.0 \pm 0.5$	1220/132
(2c)	$12.06 \pm 0.05$	$0.119 \pm 0.005$	$(3.1 \pm 0.4) \cdot 10^6$	$-9.36 \pm 0.10$	1303/132
(2d)	$11.4 \pm 1.0$	$0.05 \pm 0.11$	$0.017 \pm 0.011$	–	29/26

**Table 2.** Predictions for nuclear slope based on the parameterizations (2a) – (2d) for low  $|t|$  domain

Fitting function	Facility energies, $\sqrt{s}$										
	FAIR, GeV				NICA, GeV		RHIC, TeV		LHC, TeV		
	3	5	6.5	14.7	20	25	0.2	0.5	14	28	42*
(2a)	–	11.38	11.61	12.31	11.66	11.90	14.15	15.15	18.76	19.51	19.95
(2b)	12.57	12.80	12.93	13.32	11.67	11.91	14.02	14.94	18.28	18.97	19.37
(2c)	12.59	12.83	12.95	13.34	11.65	11.90	14.22	15.25	18.96	19.74	20.19
(2d)	–	11.90	12.01	12.43	11.70	11.96	15.00	16.67	24.44	26.39	27.58

\*The ultimate energy upgrade of LHC project [14].

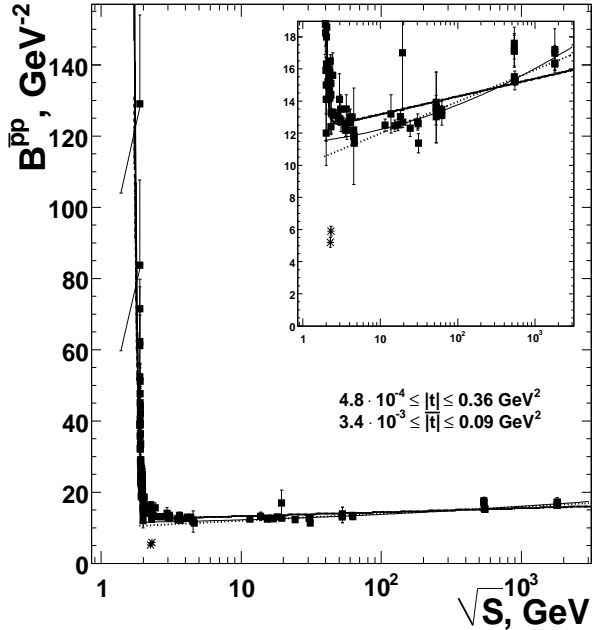


**Fig. 2.** Energy dependence of the elastic slope parameters for antiproton-proton scattering for low  $|t|$  domain. Experimental fitted points are indicated as  $\blacksquare$ , unfitted points are indicated as  $*$ . The correspondence of curves to the fit functions is the same as previously. The inner picture shows the experimental data and fits at the same scale as well as for fig.1

Our prediction with (2d) function for ultimate energy of LHC agrees well with early prediction for close SSC energy based only on slope data in the region  $5 < \sqrt{s} < 62$  GeV [4]. It should be emphasized that the fits (2a) – (2c) of available experimental data predict the slower increasing of  $B$  with energy than most of phenomenological models [15]. The  $B$  values predicted for LHC at  $\sqrt{s} = 14$  TeV by (2a) and (2c) are most close to the some model expectations [16,17]. Moreover one needs to emphasize that the model estimates at  $\sqrt{s} = 14$  TeV were obtained for  $B(t=0)$  and the  $t$ -dependence of slope shows the slight decreasing of  $B$  at growth of momentum transfer up to  $|t| \approx 0.1 - 0.2$  GeV<sup>2</sup> in particular for the models [16,17]. Thus one can expect the some better agreement between model estimations and predicted values of  $B$  from Table 2 for finite (non-zero) low  $|t|$  values. Possibly the saturation regime, Black Disk Limit, will be reached at the LHC. The one of the models in which such effects appear, namely, DDM predicts the slope  $B(t=0) \approx 23$  GeV<sup>-2</sup> at  $\sqrt{s} = 14$  TeV [18].

## 2.2 Intermediate $|t|$ domain

As indicated above the situation is more complicated for intermediate  $|t|$  domain. Differential cross section is approximated by linear,  $\ln(d\sigma/dt) \propto (-B|t|)$ , or / and quadratic,  $\ln(d\sigma/dt) \propto (-B|t| \pm Ct^2)$ , function in various experiments,  $|t|$  ranges used for  $d\sigma/dt$  approximations differ significantly etc. For quadratic exponential parametrization the  $B$  and  $C$  parameters are highly correlated by fits.

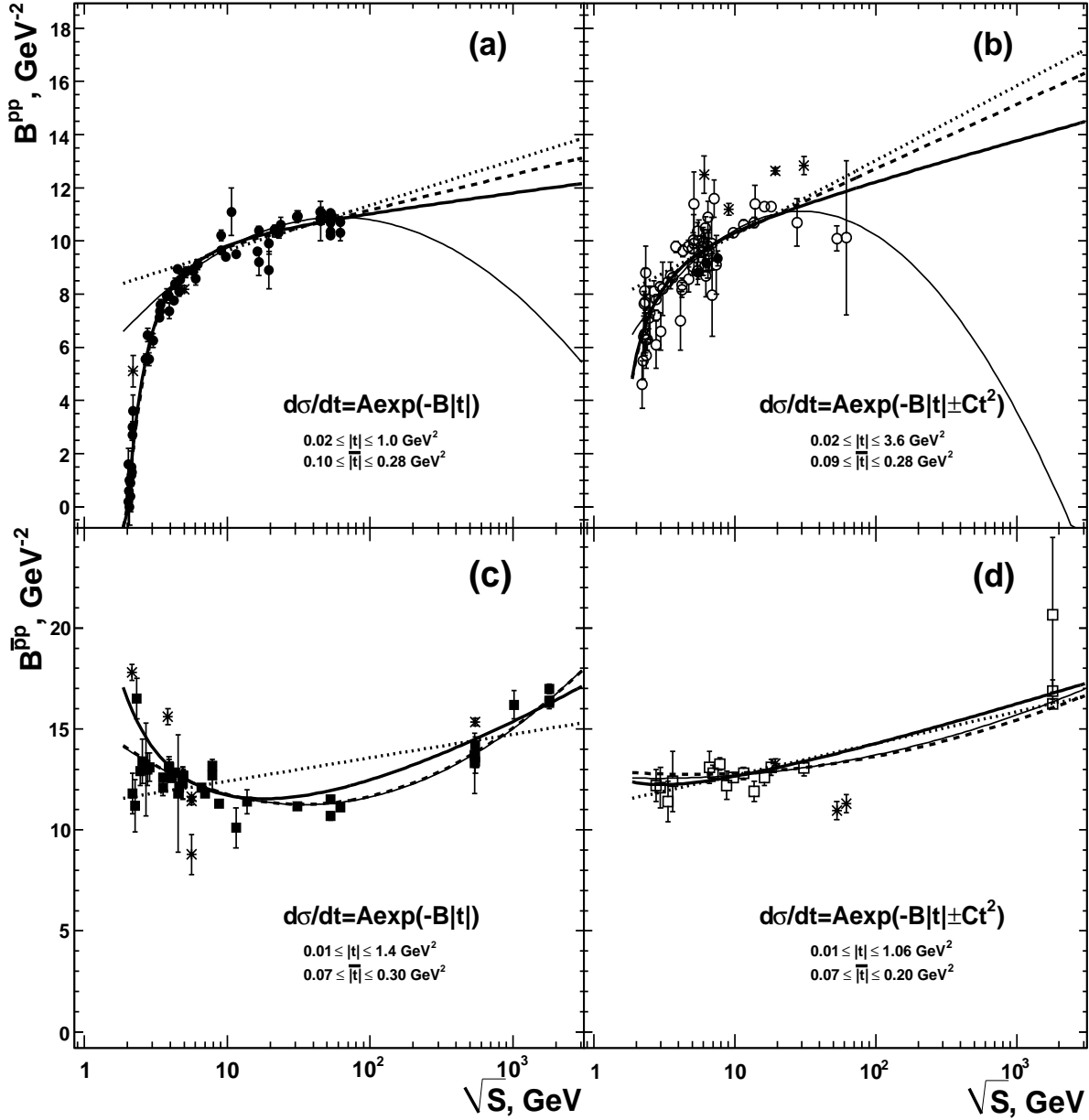


**Fig. 3.** Energy dependence of  $B$  in proton-proton (a,b) and proton-antiproton (c,d) elastic scattering for linear (a,c) and quadratic (b,d) exponential parametrization of differential cross section. Experimental points are indicated as close / open circles (squares) for  $pp$  ( $\bar{p}p$ ) for (a,c) / (b,d), unfitted points are indicated as \*. The correspondence of curves to the fit functions is the same as previously

Figure 3 shows the experimental data and corresponding fits for slope parameter energy dependence at intermediate  $|t|$  for  $pp$  and  $\bar{p}p$  elastic scattering. The Fig.3a and Fig.3c correspond to the linear exponential approximation of differential cross-section for  $pp$  and  $\bar{p}p$  respectively. Experimental data obtained at quadratic exponential fit of  $d\sigma/dt$  and fitting functions (2a) – (2d) are presented at Fig.3b for  $pp$  and at Fig.3d for  $\bar{p}p$  collisions. The fit-

ting parameter values are indicated in Table 3 for various interaction types and for different  $d\sigma/dt$  parameterizations. Usually the fit qualities are poorer for intermediate  $|t|$  values than that for low  $|t|$  range in  $pp$  elastic collisions for linear exponential parameterization of  $d\sigma/dt$ . The fitting functions (2a) and (2d) agree with experimental points qualitatively both for linear (Fig.3a) and quadratic (Fig.3b) exponential parameterizations of  $d\sigma/dt$

for  $\sqrt{s} \geq 5$  GeV only. The "expanded" functions (2b), (2c) approximate experimental data at all energies reasonably with very close fit qualities. But the (2b) function shows a very slow growth of slope parameter with energy increasing at  $\sqrt{s} \geq 100$  GeV (Fig.3a). It should be stressed that the fitting function (2d) predicts decreasing of the nuclear slope in high energy domain. Such behavior is opposite the other fitting function (2a) – (2c). In the case of linear exponential approximation of  $d\sigma/dt$  mean value of characteristic (4) is about 5.3 for excluded  $pp$  data points with (2b) function and  $\bar{n}_\chi \simeq 2.6$  for points excluded from  $\bar{p}p$  fitted data sample for (2d) fitting function.

One can see that the  $\bar{p}p$  experimental data admit the approximation by (2d) for all energy range but not only for  $\sqrt{s} \geq 5$  GeV. Indeed the fit quality for the first case much better than for second one. Additional analysis demonstrated just the same behavior of fit quality for function (2a) too. Thus  $\bar{p}p$  experimental points from linear exponential parametrization of differential cross-section are fitted by (2a) and (2d) at all energies not only for  $\sqrt{s} \geq 5$  GeV. The parameter values are shown in Table 3 for approximation by (2a), (2d) of all available experimental data. The  $\bar{p}p$  data disagreement with Regge-inspired fitting function very significantly (Fig.3c). Functions (2c) and (2d) show a very close behavior at all energies for  $\bar{p}p$  data from linear parametrization of  $\ln d\sigma/dt$ . These fitting functions have a better fit quality than (2b) but fits (2c), (2d) are still statistically unacceptable. As previously experimental data at Fig.3d allow the approximation by (2a) and (2d) for all energy range but not only for  $\sqrt{s} \geq 5$  GeV. The fit qualities are better in the first case of energy range and fitting parameters are indicated in the Table 3 for this energy range namely. As above the functions (2c) and (2d) show a close fit quality which is some better than this parameter for (2b) fitting function. One can see the fit qualities for (2a) – (2d) are better significantly for data from quadratic exponential parametrization of differential cross-sections than for data from linear exponential approximation of  $d\sigma/dt$ . Thus fitting functions (2c), (2d) agree with data points at quantitative level for quadratic (Fig.3d) parametrization of proton-antiproton  $\ln d\sigma/dt$  and these fits are statistically acceptable. Excluded points are characterized by  $\bar{n}_\chi \simeq 17.9$  for  $pp$  data with (2b) fitting function and by  $\bar{n}_\chi \simeq 12.1$  for  $\bar{p}p$  data sample at (2d) function.

From the quadratic exponential parametrization of differential cross-section one may compute the local slope at a certain  $|t|$ -value via the following relation

$$b(s, t) = B \pm C \ln |t|, \quad B, C > 0 \quad (5)$$

This characteristic can be useful for elastic scattering for study of  $d\sigma/dt$  in wider  $|t|$  range. It is suggested  $b \geq 0$  according to the definition (5). The  $b$ -parameter is named slope too, it is evaluated at  $|t| = 0.2$  GeV<sup>2</sup> usually. One of the advantages of this characteristic is the expectation of more smooth energy (momentum) dependence than that for  $B$ -parameter discussed above. Indeed we have included the 100% of available experimental points in fitted sample for  $pp$  elastic scattering. But the number of points is some

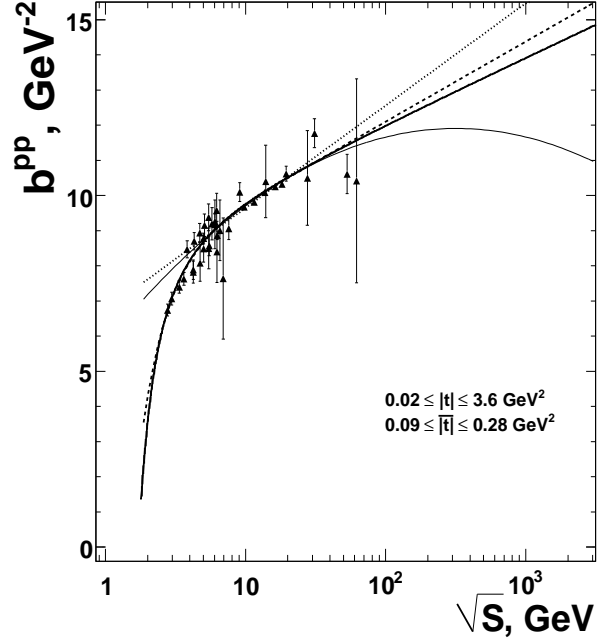


Fig. 4. Energy dependence of the slope parameter  $b$  at  $|t| = 0.2$  GeV<sup>2</sup> for proton-proton scattering. The correspondence of curves to the fit functions is the same as previously

smaller than that for  $B$ -parameter because of absent  $C$ -parameter values for some low energy measurements from [6]. We excluded one point at  $\sqrt{s} = 1.8$  TeV [19] from fitted sample for  $\bar{p}p$  elastic reaction because there are unacceptably large errors (relative error is  $\delta b \simeq 2.72$ ) for this point.

Experimental values of  $b$  depend on energy collisions and corresponding fits are shown at Fig.4 for  $pp$  elastic scattering and at Fig.5 for  $\bar{p}p$  collisions. In the last case fit qualities for (2a), (2d) functions are better for fitting at  $\sqrt{s} \geq 5$  GeV only than that for fitting of all available energy domain. The fit parameter values are shown in Table 4. Fit qualities are better significantly than that for corresponding fits of  $B$  parameter with the exception of (2a) for  $\bar{p}p$  data. Functions (2a), (2d) approximate  $b(\sqrt{s})$  for  $pp$  data statistically acceptable for  $\sqrt{s} \geq 5$  GeV only. Functions (2b) and (2c) show acceptable close fit qualities and difference at high energies only. The shrinkage parameter  $a_1^{pp}$  for best approximation function (2c) is in a good agreement with a early results [5]. Function (2b) shows a best fit quality for  $\bar{p}p$  data. Thus the "expanded" parameterizations (2b) and (2c) suppose statistically acceptable representation of all available experimental data for  $b$  parameter both in  $pp$  and  $\bar{p}p$  elastic reactions.

We have obtained predictions for nuclear slope parameters  $B$  and  $b$  for some facilities based on the fit results shown above. The predicted  $B$  values at intermediate  $|t|$  are calculated on the base of fitting parameters obtained for linear exponential parametrization of  $d\sigma/dt$ . Slope values are shown in the Table 5 for different energies of FAIR, NICA, RHIC, and LHC. According to the fit range function (2a) can predicts the  $B$  value for  $\bar{p}p$  scattering at all

**Table 3.** Fitting parameters for slope energy dependence at intermediate  $|t|$ 

Function	Parameter				
	$B_0, \text{GeV}^{-2}$	$a_1, \text{GeV}^{-2}$	$a_2, \text{GeV}^{-2}$	$a_3$	$\chi^2/\text{n.d.f.}$
proton-proton scattering, experimental data for $d\sigma/dt = A \exp(-B t )$					
(2a)	$7.95 \pm 0.12$	$0.184 \pm 0.009$	–	–	110/34
(2b)	$9.7 \pm 0.3$	$0.08 \pm 0.02$	$-22.1 \pm 1.4$	$-2.34 \pm 0.12$	240/60
(2c)	$8.51 \pm 0.14$	$0.144 \pm 0.010$	$-71 \pm 5$	$-1.49 \pm 0.06$	240/60
(2d)	$4.9 \pm 0.6$	$0.73 \pm 0.10$	$-0.09 \pm 0.02$	–	81/33
proton-proton scattering, experimental data for $d\sigma/dt = A \exp(-B t  \pm Ct^2)$					
(2a)	$7.4 \pm 0.2$	$0.31 \pm 0.03$	–	–	115/33
(2b)	$9.6 \pm 2.4$	$0.16 \pm 0.13$	$-7.2 \pm 5.4$	$-1.5 \pm 1.0$	227/62
(2c)	$7.9 \pm 0.5$	$0.26 \pm 0.05$	$-23 \pm 16$	$-1.5 \pm 0.5$	228/62
(2d)	$4.1 \pm 0.9$	$1.0 \pm 0.2$	$-0.15 \pm 0.04$	–	102/32
proton-antiproton scattering, experimental data for $d\sigma/dt = A \exp(-B t )$					
(2a)	$11.25 \pm 0.06$	$0.126 \pm 0.004$	–	–	1111/41
(2b)	$(-5.0 \pm 0.9) \cdot 10^3$	$0.64 \pm 0.02$	$(5.1 \pm 0.9) \cdot 10^3$	$(-1.5 \pm 0.3) \cdot 10^{-3}$	355/39
(2c)	$-893 \pm 69$	$5.9 \pm 0.3$	$908 \pm 69$	$(-1.44 \pm 0.06) \cdot 10^{-2}$	199/39
(2d)	$15.46 \pm 0.15$	$-0.59 \pm 0.02$	$0.083 \pm 0.003$	–	197/40
proton-antiproton scattering, experimental data for $d\sigma/dt = A \exp(-B t  \pm Ct^2)$					
(2a)	$11.1 \pm 0.2$	$0.171 \pm 0.011$	–	–	17.3/15
(2b)	$(-1 \pm 3) \cdot 10^3$	$0.26 \pm 0.06$	$(1 \pm 3) \cdot 10^3$	$(-1 \pm 4) \cdot 10^{-3}$	14.5/13
(2c)	$(-2.2 \pm 1.8) \cdot 10^2$	$1.7 \pm 0.8$	$(2.3 \pm 1.8) \cdot 10^2$	$-0.015 \pm 0.006$	13.2/13
(2d)	$12.7 \pm 0.8$	$-0.05 \pm 0.11$	$0.023 \pm 0.011$	–	13.2/14

**Table 4.** Fitting parameters for  $b$  energy dependence

Function	Parameter				
	$B_0, \text{GeV}^{-2}$	$a_1, \text{GeV}^{-2}$	$a_2, \text{GeV}^{-2}$	$a_3$	$\chi^2/\text{n.d.f.}$
proton-proton scattering					
(2a)	$6.7 \pm 0.2$	$0.32 \pm 0.02$	–	–	25.6/25
(2b)	$8.4 \pm 0.4$	$0.20 \pm 0.03$	$-10.4 \pm 1.4$	$-2.0 \pm 4.5$	41.5/33
(2c)	$7.6 \pm 0.8$	$0.25 \pm 0.07$	$-20 \pm 15$	$-1.2 \pm 0.4$	41.4/33
(2d)	$5.8 \pm 0.9$	$0.5 \pm 0.2$	$-0.05 \pm 0.04$	–	24.3/24
proton-antiproton scattering					
(2a)	$9.2 \pm 0.2$	$0.22 \pm 0.02$	–	–	40.5/13
(2b)	$-234 \pm 143$	$0.71 \pm 0.07$	$252 \pm 152$	$-0.04 \pm 0.02$	8.8/15
(2c)	$2.4 \pm 1.6$	$0.46 \pm 0.11$	$18.5 \pm 2.3$	$-0.29 \pm 0.11$	9.0/15
(2d)	$14 \pm 1$	$-0.47 \pm 0.12$	$0.07 \pm 0.01$	–	8.1/12

**Table 5.** Predictions for slope parameters based on the functions (2a) - (2d) for intermediate  $|t|$  domain

Fitting function	Facility energies, $\sqrt{s}$											
	FAIR, GeV			NICA, GeV		RHIC, TeV		LHC, TeV				
	3	5	6.5	14.7	20	25	0.2	0.5	14	28	42*	
$B$ -parameter												
(2a)	11.80	12.06	12.19	12.60	10.15	10.32	11.85	12.52	14.98	15.45	15.79	
(2b)	14.08	12.56	12.12	11.52	10.31	10.43	11.26	11.57	12.64	12.86	12.98	
(2c)	13.29	12.52	12.19	11.50	10.23	10.36	11.56	12.09	14.01	14.41	14.64	
(2d)	13.26	12.51	12.19	11.50	10.45	10.61	10.38	9.30	0.33	-2.53	-4.36	
$b$ -parameter												
(2a)	10.00	10.46	10.70	11.43	10.52	10.81	13.44	14.60	18.81	19.68	20.20	
(2b)	14.49	12.60	12.03	11.24	10.50	10.72	12.55	13.32	16.05	16.61	16.94	
(2c)	14.22	12.65	12.10	11.22	10.49	10.72	12.79	13.69	16.99	17.67	18.08	
(2d)	12.56	11.99	11.76	11.30	10.50	10.72	11.87	11.87	9.27	8.22	7.52	

\*The ultimate energy upgrade of LHC project [14].

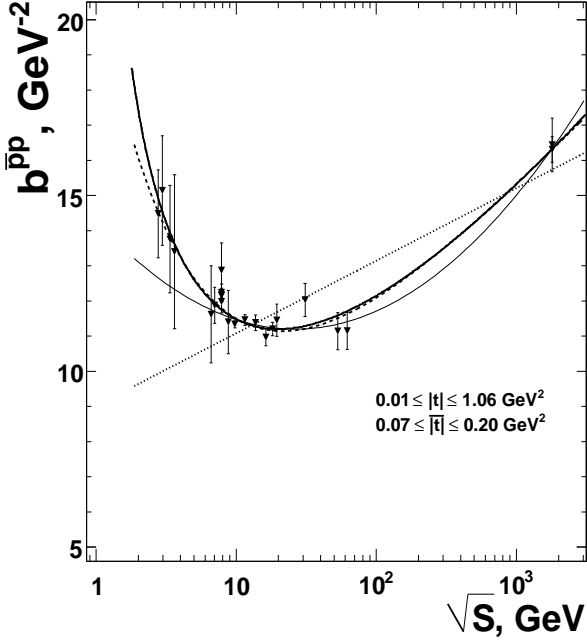


**Fig. 5.** Energy dependence of the slope parameter  $b$  at  $|t| = 0.2$   $\text{GeV}^2$  for antiproton-proton scattering. The correspondence of curves to the fit functions is the same as previously

energies under study not in  $\sqrt{s} \geq 5$  GeV domain only. As expected the functions (2c) and (2d) predicted very close slope parameter values for FAIR. All fitting functions, especially (2b) and (2c), predict the close values for nuclear slope in NICA energy domain. Functions (2a) – (2c) predict larger values for  $B$  in high-energy  $pp$  collisions than (2d) approximation. Perhaps, the future more precise RHIC results will be useful for discrimination of fitting functions under study for intermediate  $|t|$  values. The function (2d) with obtained parameters predicts negative  $B$  values at future LHC energies. It should be emphasized that various phenomenological models predict a very sharp decreasing of nuclear slope in the range  $|t| \sim 0.3\text{--}0.5$   $\text{GeV}^2$  at LHC energy  $\sqrt{s} = 14$  TeV [11]. Just the negative  $B$  value predicted for LHC at  $\sqrt{s} = 14$  TeV by (2d) is most close to the some model expectations [17, 20]. Taking into account predictions in Table 2 based on the fitting functions (2a) – (2d) for low  $|t|$  one can suggest that the model with hadronic amplitude corresponding to the exchange of three pomerons [15, 17] describes the nuclear slope some closer to the experimentally inspired values at LHC energy both at low and intermediate  $|t|$  than other models. One can see the functions (2b) and (2c) predict very close values of  $b$  up to LHC energies. Function (2d) shows a much slower decreasing of  $b$  at LHC energy domain than that for  $B$  parameter. The values of  $b$  parameter differ significantly from each other for various fitting functions in ultra-high energy domain for  $pp$  collisions and at low energies for  $\bar{p}p$  elastic scattering. It seems  $b$  parameter is more perspective for distinguishing of Regge-inspired function (2a) from “expanded” parameterizations (2b), (2c) at  $\sqrt{s} \geq 0.5$

TeV than  $B$  because of larger differences between predictions of  $b$  for corresponding functions.

### 2.3 $\Delta B$ and $NN$ data analysis

Phenomenological models predicts the zero difference of slopes ( $\Delta B$ ) for proton-antiproton and proton-proton elastic scattering at asymptotic energies. Here the difference  $\Delta B$  is calculated for each function (2a) – (2d) under study with parameters corresponded  $\bar{p}p$  and  $pp$  fits:  $\Delta B_i(s) = B_i^{\bar{p}p}(s) - B_i^{pp}(s)$ ,  $i = 2a, \dots, 2d$ . It should be stressed that the equal energy domain are used in  $\bar{p}p$  and  $pp$  fits for  $\Delta B$  calculations, i.e. the parameter values obtained by (2d) fitting function for  $\bar{p}p$  data from linear exponential fit of  $d\sigma/dt$  for  $\sqrt{s} \geq 5$  GeV are used for corresponding  $\Delta B$  definition. The energy dependence of  $\Delta B$  is shown at Fig.6a and Fig.6b for low and intermediate  $|t|$  respectively. One can see that the difference of slopes decreasing with increasing of energy for low  $|t|$  domain (Fig.6a). At present the proton-proton experimental data at highest available energy 200 GeV don’t contradict with fast (square of logarithm of energy) increasing of slope at high energies in general case. Such behavior could be agreed with the asymptotic growth of total cross section. But on the other hand the quadratic logarithmic function (2d) leads to very significant difference  $\Delta B$  for  $\bar{p}p$  and  $pp$  scattering in high energy domain for both low (Fig.6a) and intermediate (Fig.6b) values of  $|t|$ . The only Regge-inspired function (2a) predicts the decreasing of  $\Delta B$  with energy growth at intermediate  $|t|$  (Fig.6b). The parameterizations (2b) – (2d) predict the decreasing of difference of slopes at low and intermediate energies and fast increasing of  $\Delta B$  at higher energies for intermediate  $|t|$  domain (Fig.6b). As expected the most slow changing of  $\Delta B$  is predicted by Regge-inspired function (2a) at asymptotic energies. All fitting functions with experimentally inspired parameters don’t predict the constant zero values of  $\Delta B$  at high energies. But it should be emphasized that only separate fits were made for experimental data for  $pp$  and  $\bar{p}p$  elastic reactions above. These results indicate on the importance of investigations at ultra-high energies both  $pp$  and  $\bar{p}p$  elastic scattering for many fundamental questions and predictions related to the general asymptotic properties of hadronic physics.

Also we have analyzed general data samples for  $pp$  and  $\bar{p}p$  elastic scattering. Slope parameters ( $B$  and  $b$ ) shows a different energy dependence at  $\sqrt{s} < 5$  GeV in proton-proton and antiproton-proton elastic reactions in any  $|t|$  domains under study. Thus slopes for nucleon-nucleon data are investigated only for  $\sqrt{s} \geq 5$  GeV below. We have included in fitted samples only  $pp$  and  $\bar{p}p$  points which were included in corresponding final data samples at separate study  $pp$  and  $\bar{p}p$  elastic reactions above. We did not exclude any points from  $NN$  data sample, we change only the low energy boundary for fitted domain.

<sup>2</sup> Obviously, one can suggest various combinations of fitting functions for  $\Delta B$  calculations, for example, the difference between fitting functions with best fit qualities etc.

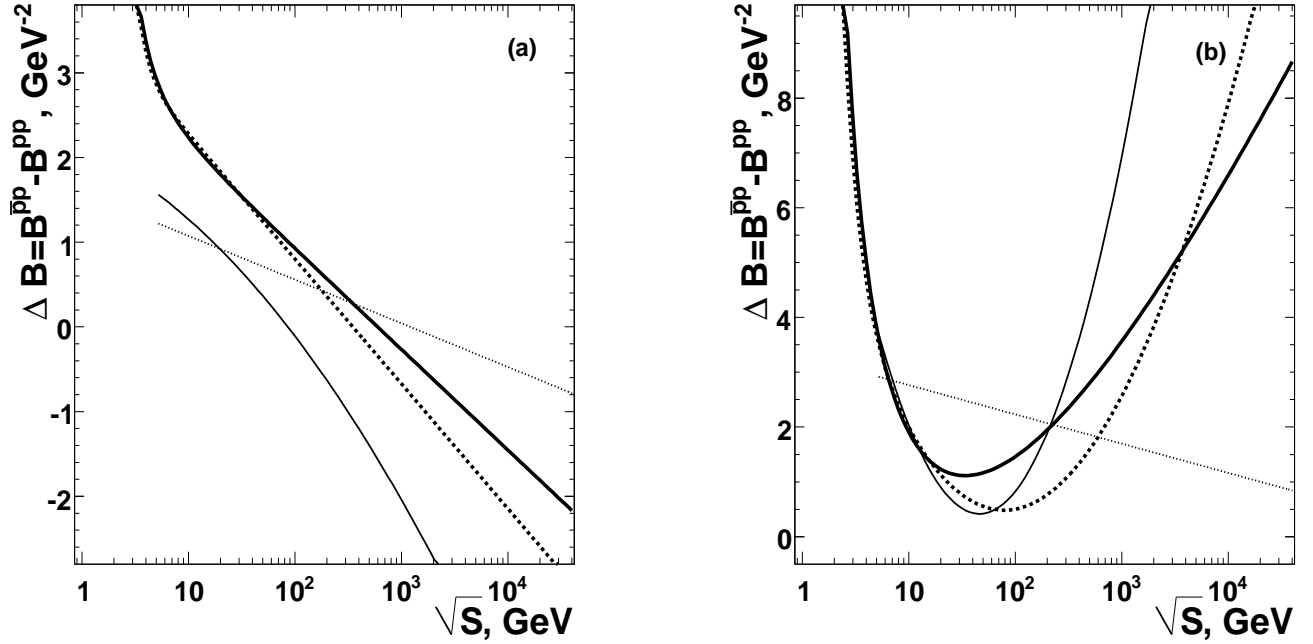


**Fig. 6.** The energy dependence of the difference of elastic slopes for proton-antiproton and proton-proton scattering in low  $|t|$  domain (a) and in intermediate  $|t|$  range for linear exponential fit of differential cross-section (b). The correspondence of curves to the fit functions is the same as above

Fig.7 shows the experimental data for slope in nucleon-nucleon elastic scattering against collision energy at low  $|t|$ . As seen from Fig.7 there is no experimental data for  $\bar{p}p$  between  $\sqrt{s} = 5$  GeV and  $\sqrt{s} = 10$  GeV. This energy domain will be available for further FAIR facility. We have fitted the general nucleon-nucleon data sample at range of low energy boundary  $s_{\min} = 25 - 400$  GeV<sup>2</sup>. The fitting parameter values are indicated in Table 6 on the first line for  $s_{\min} = 25$  GeV<sup>2</sup> and on the second one for  $s_{\min} = 400$  GeV<sup>2</sup>. The fit quality improves for all parameterizations under consideration at increasing of  $s_{\min}$ . One needs to emphasize that the fit quality is somewhat poorer ( $\chi^2/\text{n.d.f.} \approx 2.3 - 2.4$ ) at  $\sqrt{s} \geq 10$  GeV than that for  $\sqrt{s} \geq 5$  GeV for functions (2a) and (2d). In the first case the  $a_1$  parameter value is close to the Regge model prediction within errors for function (2d) only. The value  $a_1 = 0.24 \pm 0.01$  GeV<sup>-2</sup> obtained for fitting functions (2b) and (2c) at  $s_{\min} = 400$  GeV<sup>2</sup> agrees very well with the estimate for asymptotic shrinkage parameter  $\alpha'_p$ . All functions (2a) - (2d) are close to each other at energies up to  $\sqrt{s} \sim 10$  TeV at least and show quasi-linear behavior for parameter values obtained by fits with  $s_{\min} = 25$  GeV<sup>2</sup>. Fitting functions (2a) - (2d) are shown at Fig.7 for  $s_{\min} = 400$  GeV<sup>2</sup>. The function (2d) decreases at ultra-high energies  $\sqrt{s} > 20$  TeV and clear separation of various fitting functions is accessible in the LHC energy domain. We have analyzed the nucleon-nucleon data for slope parameters  $B$  and  $b$  at intermediate  $|t|$  values for linear and quadratic exponential parametrization of  $d\sigma/dt$  respectively. Fit results are shown in Table 7. Experimental  $pp$  and  $\bar{p}p$  data for  $B$  differ significantly up to  $\sqrt{s} \approx 10$  GeV at least that results in unacceptable fit qualities for

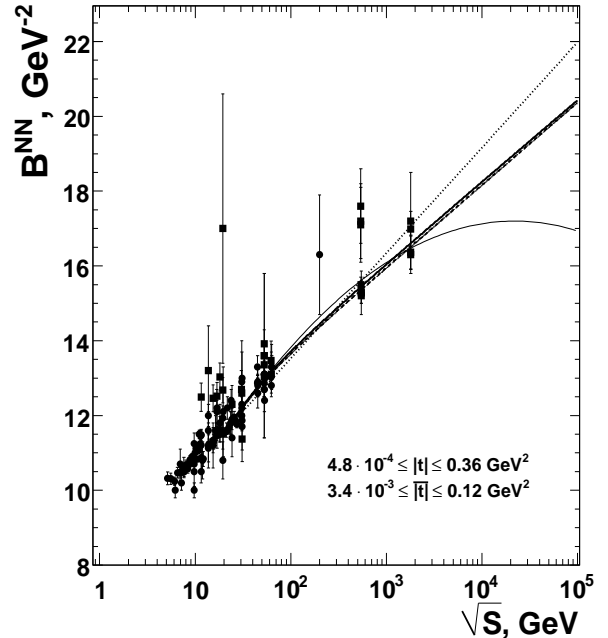


**Fig. 7.** Energy dependence of the elastic slope parameter for nucleon-nucleon scattering for low  $|t|$  domain. Experimental fitted points are indicated as  $\bullet$  for  $pp$  and as  $\blacksquare$  for  $\bar{p}p$ . Fits are shown for  $\sqrt{s_{\min}} = 20$  GeV. The correspondence of curves to the fit functions is the same as previously

all functions under study ( $\chi^2/\text{n.d.f.} \simeq 30.1$  for best fit by quadratic logarithmic function). Additional analysis demonstrate the improving of fit quality for (2b) – (2d) with increasing of low energy boundary from  $s_{\min} = 25 \text{ GeV}^2$  up to  $s_{\min} = 400 \text{ GeV}^2$ . The values of fit parameters for the last case are shown in Table 7. The Regge-inspired function (2a) contradicts with experimental data. We would like to emphasize that the best fit quality for (2a) is obtained at  $s_{\min} = 100 \text{ GeV}^2$  ( $\chi^2/\text{n.d.f.} \simeq 7.8$ ) but it is statistically unacceptable too. Functions (2b) – (2d) represent experimental  $B(\sqrt{s})$  reasonably and have a very close fit qualities. One can see from Table 7 the statistically acceptable fits have been obtained for  $b$  parameter at  $s_{\min} = 400 \text{ GeV}^2$  only. Experimental data and fit functions are presented at the Fig.8. Functions (2b) – (2d) show close fit qualities. Best fit is (2d) but "expanded" parameterizations agree with data too. One needs to emphasize the significant errors and absence of experimental points at  $\sqrt{s} \simeq 0.1 - 2 \text{ TeV}$  that trouble the more clear conclusion. The RHIC as well as LHC data for nucleon-nucleon differential cross-section at intermediate  $|t|$  will be helpful for distinguishing of various fit functions.

One can conclude the slope parameters for  $pp$  and  $\bar{p}p$  elastic scattering show universal behavior at  $\sqrt{s} \geq 20 \text{ GeV}$  and "expanded" functions represent the energy dependencies for both low and intermediate  $|t|$  ranges for this energy domain. Thus quantitative analysis of slopes at different  $|t|$  allows us to get the following estimation of low energy boundary:  $\sqrt{s} \simeq 20 \text{ GeV}$  for universality of elastic nucleon-nucleon scattering. This estimates agrees with results for differential cross-sections of  $pp$  and  $\bar{p}p$  elastic reactions based on the crossing-symmetry and derivative relations [2].

### 3 Conclusions

The main results of this paper are the following. Slope energy dependencies are analyzed quantitatively for elastic nucleon-nucleon scattering in various  $|t|$  domains. Most of all available experimental data for slope parameter in elastic nucleon collisions are approximated by different analytic functions.

The suggested new parameterizations allow us to describe experimental nuclear slope at all available energies in low  $|t|$  domain for  $pp$  quite reasonably. The new approximations agree with experimental  $\bar{p}p$  data at qualitative level but these fits are still statistically unacceptable because of very sharp behavior of  $B$  near the low energy limit. The best fit quality is obtained for "expanded" logarithmic function both for  $pp$  and  $\bar{p}p$  data. The obtained values of asymptotic shrinkage parameter  $\alpha'_{\mathcal{P}}$  for  $pp$  elastic scattering are larger than  $\alpha'_{\mathcal{P}}$  values for elastic  $\bar{p}p$  reactions for the same fitting functions. Various approximations differ from each other both in the low energy and very high energy domains. Predictions for slope parameter are obtained for elastic proton-proton and proton-antiproton scattering in energy domains of some facilities at low momentum transfer. Our predictions based on the

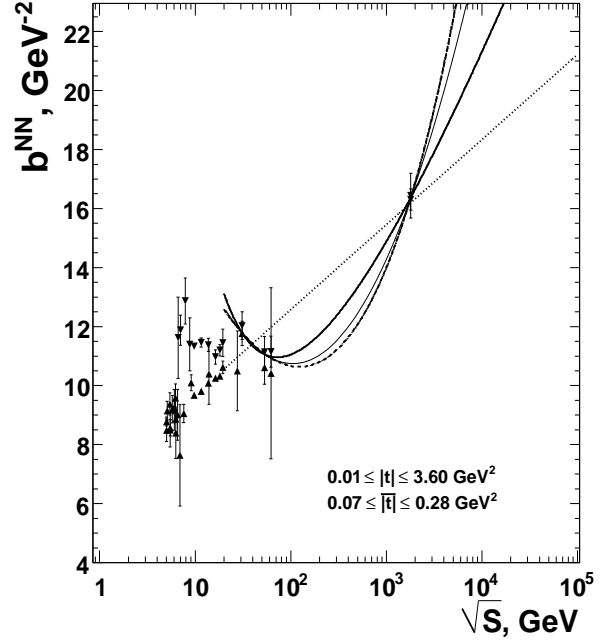


**Fig. 8.** Energy dependence of the elastic slope parameter  $b$  at  $|t| = 0.2 \text{ GeV}^2$  for nucleon-nucleon scattering for intermediate  $|t|$  domain. Experimental fitted points are indicated as  $\blacktriangle$  for  $pp$  and as  $\blacktriangledown$  for  $\bar{p}p$ . Fits are shown for  $\sqrt{s_{\min}} = 20 \text{ GeV}$ . The correspondence of curves to the fit functions is the same as previously

all available experimental data don't contradict the phenomenological model estimations qualitatively. The situation is more unclear at intermediate  $|t|$  values than for low  $|t|$  domain. Only the qualitative agreement is observed between approximations and experimental points both for  $pp$  and  $\bar{p}p$  collisions for linear exponential parametrization of  $d\sigma/dt$  because of poorer quality of data. The "expanded" logarithmic function describes of  $pp$  data for  $B$  parameter for any differential cross-section parametrization reasonably. Best fit quality is obtained for quadratic function of logarithm for  $\bar{p}p$  data. One needs to emphasize that this function allows us to describe  $\bar{p}p$  data at all available energies and shows a statistically acceptable fit quality for data sample obtained from quadratic exponential parametrization of  $d\sigma/dt$ . Slope parameter  $b$  calculated at  $|t| = 0.2 \text{ GeV}^2$  shows more smooth energy dependence. We have obtained an acceptable fit qualities for "expanded" functions both for  $pp$  and  $\bar{p}p$  data at all initial energies. The obtained values of asymptotic shrinkage parameter  $\alpha'_{\mathcal{P}}$  for  $pp$  elastic scattering are close to the early results both in low and intermediate  $|t|$  domain. As well as for low  $|t|$  domain predictions for slope parameters  $B$  and  $b$  are obtained for elastic proton-proton and proton-antiproton scattering in energy domains of some facilities. It seems the phenomenological model with hadronic amplitude corresponding to the exchange of three pomerons describes the nuclear slope some closer to the experimental fit inspired values at LHC energy both at low and intermediate  $|t|$  than other models.

**Table 6.** Fitting parameters for slope energy dependence in low  $|t|$  domain for  $NN$  elastic scattering

Function	Parameter				
	$B_0, \text{GeV}^{-2}$	$a_1, \text{GeV}^{-2}$	$a_2, \text{GeV}^{-2}$	$a_3$	$\chi^2/\text{n.d.f.}$
(2a)	$8.35 \pm 0.06$	$0.278 \pm 0.005$	–	–	272/124
	$7.89 \pm 0.11$	$0.306 \pm 0.008$	–	–	82.8/60
(2b)	$8.21 \pm 0.07$	$0.285 \pm 0.005$	$1.6 \pm 0.4$	$-2.0 \pm 2.4$	271/122
	$9.54 \pm 0.25$	$0.24 \pm 0.01$	$-514 \pm 244$	$-3.5 \pm 0.3$	59.1/58
(2c)	$8.05 \pm 0.55$	$0.29 \pm 0.02$	$0.64 \pm 0.55$	$-0.3 \pm 0.4$	270/122
	$9.3 \pm 0.2$	$0.24 \pm 0.01$	$-43 \pm 18$	$-0.67 \pm 0.08$	59.1/58
(2d)	$8.48 \pm 0.14$	$0.26 \pm 0.02$	$(3 \pm 3) \cdot 10^{-3}$	–	271/123
	$5.6 \pm 0.5$	$0.58 \pm 0.06$	$-0.029 \pm 0.006$	–	61.1/59

**Table 7.** Fitting parameters for energy dependence of slope parameters at intermediate  $|t|$  for  $NN$  elastic scattering

Function	Parameter				
	$B_0, \text{GeV}^{-2}$	$a_1, \text{GeV}^{-2}$	$a_2, \text{GeV}^{-2}$	$a_3$	$\chi^2/\text{n.d.f.}$
	<i>B</i> -parameter				
(2a)	$5.44 \pm 0.12$	$0.352 \pm 0.007$	–	–	268/31
(2b)	$-242 \pm 43$	$1.00 \pm 0.05$	$267 \pm 45$	$-0.06 \pm 0.01$	110/31
(2c)	$-135.9 \pm 0.5$	$2.31 \pm 0.06$	$151.0 \pm 0.7$	$-0.040 \pm 0.002$	102/31
(2d)	$14.1 \pm 0.7$	$-0.52 \pm 0.07$	$0.081 \pm 0.006$	–	101/32
	<i>b</i> -parameter				
(2a)	$6.97 \pm 0.13$	$0.318 \pm 0.012$	–	–	221/40
	$6.8 \pm 0.5$	$0.31 \pm 0.03$	–	–	15.3/7
(2b)	$7.5 \pm 0.2$	$0.282 \pm 0.017$	$-595 \pm 662$	$-6 \pm 3$	206/38
	$-23 \pm 8$	$0.98 \pm 0.19$	$144 \pm 40$	$-1 \pm 2$	2.43/5
(2c)	$7.5 \pm 0.2$	$0.281 \pm 0.016$	$-152 \pm 287$	$-1.7 \pm 0.6$	205/38
	$9.0 \pm 28.5$	$-1.7 \pm 1.4$	$13 \pm 31$	$0.10 \pm 0.08$	2.40/5
(2d)	$6.5 \pm 0.3$	$0.40 \pm 0.04$	$-0.010 \pm 0.005$	–	217/39
	$26 \pm 5$	$-1.6 \pm 0.5$	$0.17 \pm 0.05$	–	2.40/6

The energy dependence of difference of slopes ( $\Delta B$ ) for proton-antiproton and proton-proton elastic scattering was obtained for fitting functions under study. The  $\Delta B$  parameter shows the opposite behaviors at high energies for low and intermediate  $|t|$  domains (decreasing / increasing, respectively) for all fitting functions with the exception of Regge-inspired one. The last function predicts the slow decreasing of  $\Delta B$  with energy growth. It should be emphasized that all underlying empirical fitting functions with experimentally inspired parameter values don't predict the zero difference of slopes for proton-antiproton and proton-proton elastic scattering both at low and intermediate  $|t|$  for high energy domain. We have analyzed general nucleon-nucleon data samples for slopes at  $\sqrt{s} \geq 5$  GeV. The "expanded" functions show the best and statistically acceptable fit qualities at  $\sqrt{s} \geq 20$  GeV for low  $|t|$  domain. Slope analysis allows us to find the following value  $0.24 \pm 0.01$  for  $\alpha'_p$  parameter. The estimation of asymptotic shrinkage parameter  $\alpha'_p$  obtained with "expanded" functions for  $NN$  data agree very well with Pomeron theory expectation. The quadratic logarithmic function represents experimental  $NN$  data for  $B$  and  $b$  slope parameters with best quality. But the functions (2b) and (2c) show a close qualities and agree with data reasonably. Therefore suggested "expanded" functions can be used as a reliable fits for wide range of momentum transfer at all

energies. The universal behavior was found for available experimental  $pp$  and  $\bar{p}p$  slopes at  $\sqrt{s} \geq 20$  GeV both for low and intermediate  $|t|$  that is in agreement with the hypothesis of a universal shrinkage of the hadronic diffraction cone at high energies.

## References

1. R.F. Ávila, S.D. Campos, M.J. Menon, J. Montanha, Eur. Phys. J. C **47**, 171 (2006).
2. S.B. Nurushev, and V.A. Okorokov, Proceedings of the XII Advanced Research Workshop on High Energy Spin Physics, JINR, Dubna, 3-7 September 2007, A.V. Efremov and S.V. Goloskokov (Eds.), (JINR, Dubna, 2008), pp. 117-121; 0711.2231[hep-ph].
3. V.A. Okorokov, 0811.0895[hep-ph], 0811.3849[hep-ph].
4. M.M. Block, and R.N. Cahn, Rev. Mod. Phys. **57**, 563 (1985).
5. J.P. Burq, et al., Nucl. Phys. B **217**, 285 (1983).
6. T. Lasinski, et al., Nucl. Phys. B **37**, 1 (1972).
7. I. Ambast, et al., Phys. Rev. D **9**, 1179 (1974).
8. P. Jenni, et al., Nucl. Phys. B **129**, 232 (1977).
9. L.A. Fajardo, et al., Phys. Rev. D **24**, 46 (1981).
10. H. Iwasaki, et al., Nucl. Phys. A **433**, 580 (1985).
11. The Durham HEP Reaction Data Databases (UK) <http://durpdg.dur.ac.uk/hepdata/reac.html>

12. M.M. Block, Phys. Rep. **436**, 71 (2006).
13. G. Giacomelli, Phys. Rep. **23**, 123 (1976).
14. A.N. Skrinsky, Proceedings of the XXXIII International Conference of High Energy Physics, Moscow, Russia, 26 July - 2 August, 2006, A. Sissakian, G. Kozlov and E. Kolganova (Eds.), (World Scientific, 2007, **I**), pp. 175-186.
15. V. Kundrať, J. Kašpar and M. Lokajčec Proceedings of the XII International Conference on Elastic and Diffractive Scattering Forward Physics and QCD, DESY - Gamburg, Germany, 21 - 25 May, 2007, J. Bartels, M. Diehl and H. Jung (Eds.), (Verlag DESY, 2007), pp.273-278.
16. M.M. Block, E.M. Gregores, F. Halzen and G. Pancheri, Phys. Rev. D **60**, 054024 (1999).
17. V.A. Petrov, E. Predazzi and A.V. Prokhudin, Eur. Phys. J. C **28**, 525 (2003).
18. O.V. Selyugin, J.-R. Cudell, Proceedings of the XII International Conference on Elastic and Diffractive Scattering Forward Physics and QCD, DESY - Gamburg, Germany, 21 - 25 May, 2007, J. Bartels, M. Diehl and H. Jung (Eds.), (Verlag DESY, 2007), pp.279-284.
19. N.A. Amos, et al., Phys. Lett. B **247**, 127 (1990).
20. C. Bourrely, J. Soffer and T.T. Wu, Eur. Phys. J. C **28**, 97 (2003).